Stability and Selective Oxidation of Aluminum in Nano-Laminate Ti_3AlC_2 upon Heating in Argon

X. H. Wang and Y. C. Zhou*

High-Performance Ceramic Division, Shenyang National Laboratory for Materials Science, Institute of Metal Research, Chinese Academy of Sciences, 72 Wenhua Road, Shenyang 110016, P. R. China

Received January 8, 2003. Revised Manuscript Received July 9, 2003

Nano-laminate Ti_3AlC_2 is a layered ternary carbide consisting of periodic planar stacking of edge-sharing Ti_6C octahedra and close-packed Al atoms along the *c*-axis. Ti_3AlC_2 has a unique combination of interesting properties that make it a promising candidate material in diverse applications. In this paper, the stability of nano-laminate Ti_3AlC_2 upon heating in argon with low oxygen content has been investigated. It was indicated that nano-laminate Ti_3AlC_2 was stable below at least 1460 °C. On the other hand, selective oxidation of Al in Ti_3AlC_2 took place on top of the specimen, which resulted in the transformation of Ti_3AlC_2 into substoichiometric TiC_x and Al_2O_3. Aligned submicropores were observed on the oxidized particles. Those pores were regarded as the rapid channels through which alumium atoms could easily migrate outward from the substrate to form protective Al_2O_3 scales on bulk Ti_3AlC_2 at high temperatures. Because of the synergic and whole migration of Al atoms, there was no Al-depletion area beneath the protective scales.

1. Introduction

Ti_3AlC_2 is a layered machinable ternary carbide identified by Pietzka and Schuster in 1994.[1] It crystallizes as a hexagonal structure with a space group of $P6_3/mmc$ with lattice parameters of $a = 0.30753$ nm and $c = 1.8578$ nm. Its structure can be described as periodic planar stacking of sheets of edge-sharing Ti_6C octahedra and close-packed Al atoms along the *c*-axis. The atoms are located in the following Wyckoff positions: 4 Ti atoms at 4*f* ($z = 0.1280$); 2 Ti atoms at 2*a*; 2 Al atoms at 2*b*; and 4 C atoms at 4*f* ($z = 0.5640$).[1]

Because of the layered structural feature and each sheet of edge-sharing Ti_6C octahedra and close-packed Al atoms in nano scale, Ti_3AlC_2 is also included in the thermodynamically stable nano-laminates.[2] Both theoretical calculation[3] and experimental works[4,5] have demonstrated that Ti_3AlC_2 has a striking combination of characters of both ceramics and metals. Like ceramics, it has low density (4.2 g/cm^3), low thermal expansion coefficient, high modulus and high strength, and good high-temperature oxidation resistance.[6] Like metals, it is a good electrical and thermal conductor, readily machinable, tolerant to damage, and resistant to thermal shock. The unique combination of these interesting properties enables Ti_3AlC_2 to be a promising candidate material for use in diverse fields, especially in high-temperature applications. However, fundamental knowledge about the thermal stability of nano-laminate Ti_3AlC_2 is very limited. The stability of this technologically important material was simply mentioned by Pietzka et al.[1] According to them, estimation of the decomposition temperature of Ti_3AlC_2 was based on experiments in a tungsten furnace at 1360, 1430, and 1530 °C.

Meanwhile, it has been demonstrated that protective scales consisting of continuous inner Al_2O_3 layers were formed on bulk Ti_3AlC_2 and Ti_2AlC at high temperatures in air despite the low Al content in the two layered ternary carbides.[6,7] In the high-temperature oxidation of alumina-forming intermetallics and alloys such as NiAl, [8−11] FeAl,[11] FeCrAl,[12,13] TiAl,[14−16] and $TiAl_3$,[17] which have been extensively studied, Al-depletion layers were always present in the sub-scale area. However, it was surprising to note that no Al-depletion layers were observed in the sub-scale area after either bulk Ti_3AlC_2 or Ti_2AlC was exposed to air at higher temperatures of 1000−1300 °C for 20 h.[6,7]

* Corresponding author. E-mail: yczhou@imr.ac.cn.

(1) Pietzka, M. A.; Schuster, J. C. *J. Phase Equilib.* **1994**, *15*, 392.
(2) Barsoum, M. W. *Prog. Solid State Chem.* **2000**, *28*, 201.
(3) Zhou, Y. C.; Wang, X. H.; Sun, Z. M.; Chen, S. Q. *J. Mater. Chem.* **2001**, *11*, 2335.
(4) Tzenov, N. V.; Barsoum, M. W. *J. Am. Ceram. Soc.* **2000**, *83*, 825.
(5) Wang, X. H.; Zhou, Y. C. *Acta Mater.* **2002**, *50*, 3141.
(6) Wang, X. H.; Zhou, Y. C. *Corros. Sci.* **2003**, *45*, 891.
(7) Wang, X. H.; Zhou, Y. C. *Oxid. Met.* **2003**, *59*, 303.
(8) Grabke, H. J.; Steinhorst, M.; Brumm, M.; Wiemer, D. *Oxid. Met.* **1991**, *35*, 199.
(9) Nesbitt, J. A.; Vinarcik, E. J.; Barrett, C. A.; Doychak, J. *Mater. Sci. Eng. A.* **1992**, *153*, 561.
(10) Bobeth, M.; Bischoff, E.; Schumann, E.; Rockstroh, M.; Ruhle, M. *Corros. Sci.* **1995**, *37*, 657.
(11) Grabke, H. J. *Mater. Sci. Forum* **1997**, *251−2*, 149.
(12) Sarioglu, S.; Blachere, J. R.; Pettit, F. S.; Meier, G. H.; Smialek, J. L.; Mennicke, C. *Mater. Sci. Forum* **1997**, *251−2*, 405.
(13) Lesage, B.; Marechal, L.; Huntz, A. M.; Molins, R. *Defect Diffus. Forum* **2001**, *194−1*, 1707.
(14) Beye, R. W.; Gronsky, R. *Acta Metall. Mater.* **1994**, *42*, 1373.
(15) Dettenwanger, F.; Schumann, E.; Ruhle, M.; Rakowski, J.; Meier, G. H. *Oxid. Met.* **1998**, *50*, 269.
(16) Shemet, V.; Hoven, H.; Quadakkers, W. J. *Intermetallics* **1997**, *5*, 311.
(17) Smialek, J. L. *Corros. Sci.* **1993**, *35*, 1199.

10.1021/cm030022v CCC: $25.00
Published on Web 08/19/2003

Table 1. Impurities and Their Contents in Argon

O_2	N_2	H_2O	H_2	C_nH_n
12 ppm	5 ppm	8 ppm	1 ppm	2 ppm

This work has two aims: first, to investigate the stability of Ti_3AlC_2 upon heating; second, to create a circumstance with low oxygen partial pressure like that beneath the protective scales formed on either Ti_3AlC_2 or Ti_2AlC in an attempt to understand the selective oxidation of Al, as well as the absence of an Al-depletion area beneath the scales consisting of continuous inner Al_2O_3 layers on bulk Ti_3AlC_2 through heating Ti_3AlC_2 powders in argon with low oxygen content.

2. Experimental Section

In this work, monolithic Ti_3AlC_2 powders with a BET specific surface area of 2.7 m^2/g were used. The BET specific surface area measurement was conducted in an ASAP 2010 volumetric analyzer, and the specific surface area was determined by calculating the volume of absorbed nitrogen at 77 K. The Ti_3AlC_2 powders were fabricated by a novel solid−liquid reaction synthesis procedure using commercially available elemental powders of Ti, Al, and graphite as raw materials. Detailed description on the fabrication process has been published elsewhere.[18]

In a typical experiment, approximately 80 mg of Ti_3AlC_2 powder was initially loaded into an Al_2O_3 crucible with a capacity of 170 μL and then introduced into the sample chamber of a Setsys 16/18 thermoanalyzer (SETARAM, France). Prior to each simultaneous thermogravimetry/differential scanning calorimetry (TG/DSC) or TG alone test, the sample chamber was degassed for 10 min using a primary pump, and subsequently filled with argon. Leakhunting was carried out to make sure that the sample chamber was leak-free. The impurities in argon used in this study include O_2, N_2, H_2O, H_2, and C_nH_n. The impurity contents claimed by the manufacturer are listed in Table 1. To further remove the residual atmosphere in the sample chamber, another two degassing−filling procedures were repeated. The above procedures and simultaneous TG/DSC or TG alone tests were automatically carried out by a personal computer and SETARAM collection interface for data logging, and SETARAM processing interface for data analysis. No attempt was made to measure the precise content of oxygen in the sample chamber; however, its content was close to that in the argon because the sample chamber was leak-free and swept by degassing−cleaning three times. As argon flew out of the sample chamber through a nonreturn valve in the last run of filling argon, the Ti_3AlC_2 powders were heated at a rate of 10 °C/min up to 1460 °C and then cooled at the same rate to ambient temperature. The flow rate of argon was 0.75 L/hour.

To remove the false weight changes during heating and cooling (weight increases upon heating and weight decreases under cooling), blank experiments were carried out by heating Al_2O_3 powders with the same weight as the Ti_3AlC_2 powders and the curves were defined as corresponding baselines for simultaneous TG/DSC or TG alone tests. Thermal analysis results reported in this work were calibrated by subtracting the corresponding baselines.

Phase identification was conducted in a D/max 2500PC X-ray diffractometer (Rigaku, Japan) operated at 50 kV and 200 mA using Cu Kα radiation. The pattern was collected at a scanning rate of 0.4°(2θ)/min in a step of 0.02°. Morphologies of each distinct part of the heated specimens were observed in a JSM-6301F field emission scanning electron microscope with resolution of 1.5 nm (JEOL, Japan). Elemental composition analysis was performed using the energy dispersive spectroscopy (EDS) system (Oxford instruments, U.K.) equipped in the SEM. In-situ high-temperature X-ray diffraction examinations were performed in a D8 Discover diffractometer (Bruker axs, Germany). The tube voltage and tube current were operated at 40 kV and 40 mA, respectively.

(18) Wang, X. H.; Zhou, Y. C. *J. Mater. Chem.* **2002**, *12*, 455.

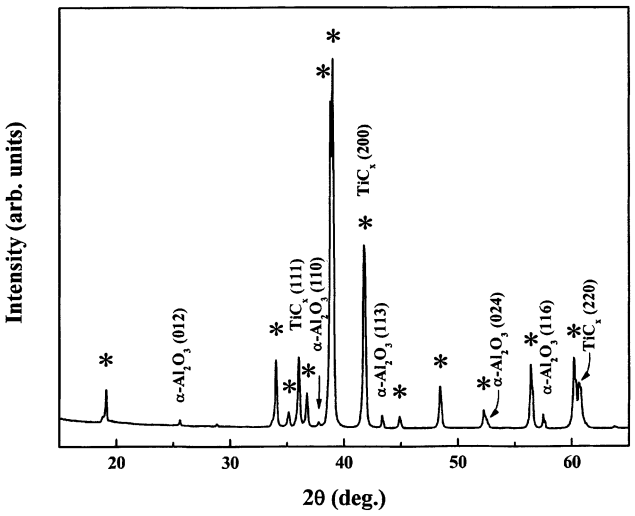

Figure 1. XRD pattern of Ti_3AlC_2 powders after heating to 1460 °C in Ar showing the predominant Ti_3AlC_2 and the coexistence of TiC_x and Al_2O_3. Diffraction peaks indicated by asterisks correspond to Ti_3AlC_2.

3. Results and Discussion

In calibrated DSC curves of Ti_3AlC_2 powders upon heating and under cooling, no obvious DSC peaks were observed, indicating that phase transformation associated with thermal effect did not occur. As the sample within the corundum crucible after heating was pulled out of the sample chamber, a white cotton-like matter was observed on top of the heated specimen. The white cotton-like matter was carefully separated with tweezers for SEM observation. In addition, after the remaining specimen was withdrawn from the Al_2O_3 crucible, it was clearly observed that the specimen after heating exhibits a macroscale layered structure: beneath the white cotton-like matter the color of the powders changed to black, while at the bottom they still kept the original light gray of Ti_3AlC_2. In another run with the identical condition, the whole specimen including the white cotton-like matter was withdrawn from the crucible and then ground slightly in an agate mortar for phase identification. According to the powder X-ray diffraction pattern shown in Figure 1, the specimen after heating in argon consists of predominant Ti_3AlC_2, indicating that it can keep its original crystal structure at temperatures up to 1460 °C. To verify the stability of Ti_3AlC_2, as well as to examine if a reversible phase transformation occurred at high temperature, in-situ high-temperature XRD analyses of Ti_3AlC_2 powders were also successively carried out under vacuum at 600, 800, 1000, 1200, 1300, 1360, and 1400 °C. The results showed that the diffraction peaks corresponding to Ti_3AlC_2 shifted to a small degree with the increase of temperature and no extra diffraction peaks were detected, which confirms that Ti_3AlC_2 is stable at least below 1400 °C and there is no reversible phase transformation upon heating to that temperature. In addition to the predominant Ti_3AlC_2 phase, other two phases of TiC_x and Al_2O_3 were identified in the sample after heating to 1460 °C in Ar (Figure 1) suggesting that

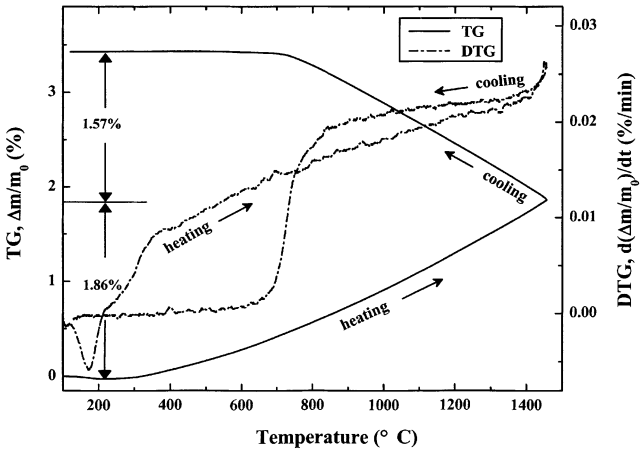

Figure 2. Calibrated thermogravimetry (TG) and differential thermogravimetry (DTG) curves of Ti_3AlC_2 powders upon heating and under subsequent cooling. TG refers to the percent of weight change (Δm) to the original weight (m_0) of the sample. DTG refers to the rate of change in the percent with time. The heating and cooling rates are 10 K/min.

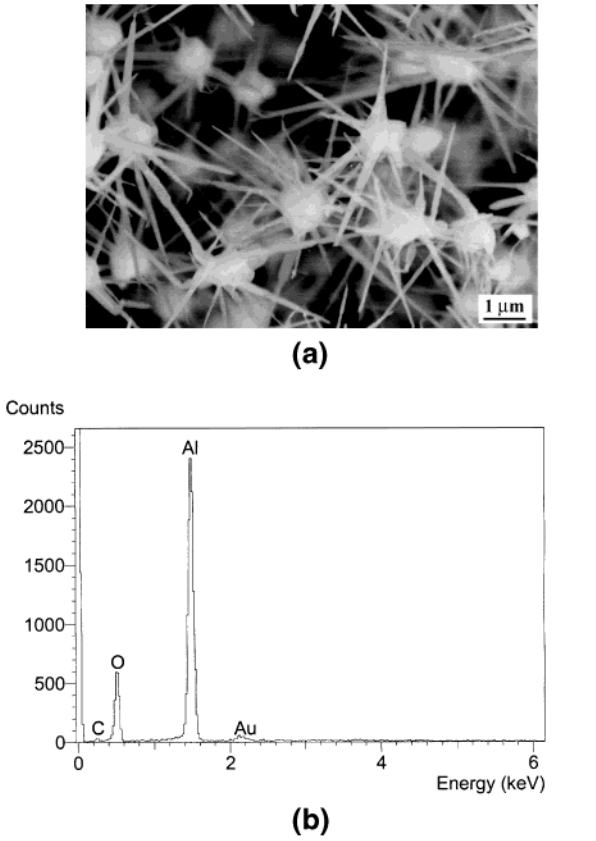

Figure 3. (a) Secondary electron image of the white cotton-like matter on top of the heated Ti_3AlC_2 powders. (b) EDS spectrum taken from the white cotton-like matter, showing that the cotton-like matter is Al_2O_3.

selective oxidation of aluminum in Ti_3AlC_2, which caused the transformation of Ti_3AlC_2 into TiC_x and Al_2O_3, occurred upon heating in Ar with low oxygen content.

It has been demonstrated that the structures and properties between another layered ternary carbide Ti_3SiC_2 and binary carbide TiC were strongly related and that the crystal structure of ternary Ti_3SiC_2 could be considered as a layer of Si atoms intercalated into (111) twin boundary of TiC.[19,20] Because Ti_3AlC_2 is isotopic with Ti_3SiC_2,[1] as a result, the crystal structure of ternary Ti_3AlC_2 can also be considered as a layer of Al atoms intercalated into (111) twin boundary of TiC. According to the powder XRD result (Figure 1), the TiC_x unit remained while Al was oxidized into Al_2O_3 after the heating of nano-laminate Ti_3AlC_2 in argon with low oxygen content. The selective reactivity of Si in Ti_3SiC_2 isotopic with Ti_3AlC_2 has been reported in the literature.[21,22] For the carburization of Ti_3SiC_2, selective removal of Si occurred.[21] The preferential reaction of

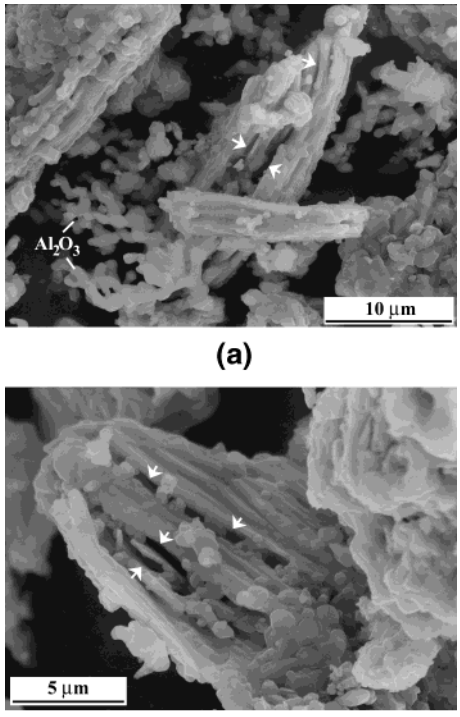

Figure 4. (a) and (b) SEM micrographs of the black particles beneath the white cotton-like matter showing that aligned submicropores indicated by arrows are distributed in the oxidized particles. In (a), antler-like Al_2O_3 grow from the oxidized particles is marked.

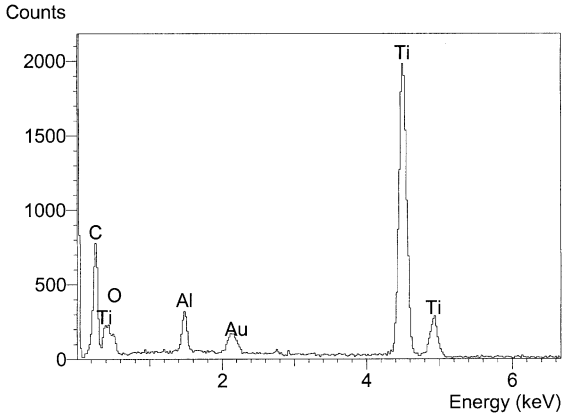

Figure 5. EDS spectrum taken from the region of oxidized particles in which aligned submicropores are distributed like those shown in Figure 4.

(19) Zhou, Y. C.; Sun, Z. M.; Yu, B. H. *Z. Metallkd.* **2000**, *91*, 937.
(20) Barsoum, M. W. *Scr. Mater.* **2000**, *43*, 285.
(21) El-Raghy, T.; Barsoum, M. W. *J. Appl. Phys.* **1998**, *83*, 112.
(22) Barsoum, M.; El-Raghy, T.; Farber, L.; Amer, M.; Christini, R.; Adams, A. *J. Electrochem. Soc.* **1999**, *146*, 3919.

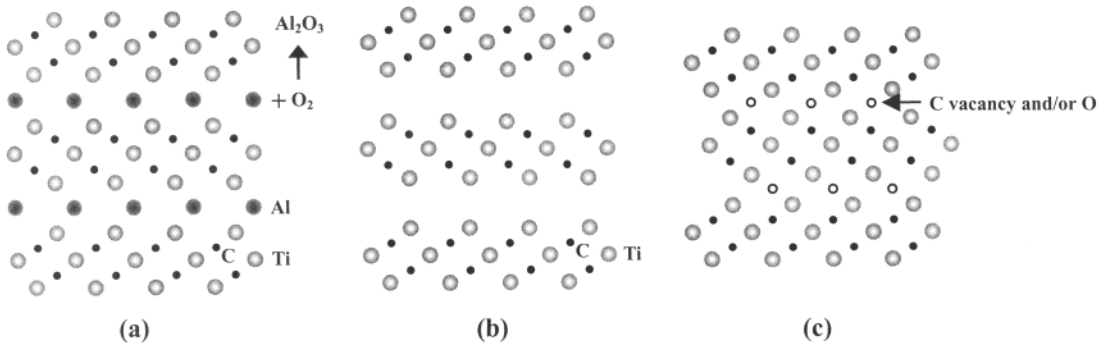

Figure 6. Idealized transformation process from Ti_3AlC_2 into titanium oxycarbide $TiC_{0.67}O_y$ owing to the selective oxidation of Al into Al_2O_3. (a) Projection of atoms on (11 $\bar{2}$0) plane of Ti_3AlC_2; (b) loss of Al in Ti_3AlC_2 gives Ti_3C_2 twins; and (c) uptake of oxygen in Ti_3C_2 twins and their reconstruction results in titanium oxycarbide $TiC_{0.67}O_y$.

Si in Ti_3SiC_2 with cryolite has also been reported by Barsoum and co-workers.[22] In the present work, as mentioned above, the transformation of Ti_3AlC_2 into TiC_x and Al_2O_3 only took place at the top of the specimen as a result of selective oxidation of aluminum. Therefore, it is reasonable to conclude that the transformation of Ti_3AlC_2 into TiC_x and Al_2O_3 was induced by the selective oxidation of aluminum in Ti_3AlC_2. The selective oxidation of Al under low oxygen partial pressure is attributed to not only its higher affinity with oxygen than the other elements of Ti and C but also the higher activity of aluminum in nano-laminate Ti_3AlC_2.

According to the thermodynamics data,[23−25] the Gibbs free energy for the reaction of Al and oxygen to form Al_2O_3 is more negative than the other reactions of Ti and C with oxygen, which suggests that aluminum has higher affinity with oxygen than the other elements of Ti and C. Because TiC survived the oxidation and it is very thermodynamically stable, the oxidation of TiC as a unit with oxygen was also considered. The Gibbs free energies for the oxidation reactions of TiC with oxygen into TiO and/or TiO_2, CO and/or CO_2 are also calculated from the thermodynamics data.[23−25] It is indicated that the Gibbs free energies for those reactions are less negative than the reactions of elements Ti and Al with oxygen to form TiO_2, TiO, or Al_2O_3, which suggests that TiC as a unit has much less affinity with oxygen than element Al. Moreover, weak bonding between Ti_6C octahedra layers and neighboring sheets of Al atoms[3] in Ti_3AlC_2 enables Al to have a high chemical activity, which is thermodynamically favorable for the selective oxidation of Al in nano-laminate Ti_3AlC_2.

In the present study, selective oxidation of Al in nano-laminate Ti_3AlC_2 occurred upon heating in argon with low oxygen partial pressure. As oxygen partial pressures were high enough like that in air for the oxidation of elements Ti, Al, and C, exposure of Ti_3AlC_2 powders to air at high temperatures would simultaneously yield the oxides of the elements, which has been confirmed by the previous work.[26] As only TiC were exposed to an Ar/O_2 atmosphere with low oxygen content (about 270 ppm) at high temperature (1073 K), it was oxidized into TiO_2 and CO_2 with retention of amorphous carbon.[27]

To measure more precisely the weight changes during heating and cooling of Ti_3AlC_2 powders in argon, the TG alone option with higher resolution was used. The TG curves of Ti_3AlC_2 powders upon heating and under cooling exhibit different characteristics as shown in Figure 2. Upon heating, the weight continuously increased with temperature with exception in the temperature range of 122−215 °C. The decrease in weight in that temperature range corresponded to desorption of water vapor adsorbed on the Ti_3AlC_2 powders. However, for the TG curve under subsequent cooling, the increase in weight abruptly stopped at about 600 °C. According to the X-ray diffraction result (Figure 1), only one oxide, Al_2O_3, was present in the sample after heating, so it is reasonable to conclude that the growth kinetics for Al_2O_3 was too slow to be detected within the resolution of the apparatus as the temperature decreased below that temperature. Whereas upon heating, the weight gain with temperature below 600 °C suggests that uptake of oxygen by Ti_3AlC_2 occurred. The "fresh" surface of Ti_3AlC_2 powders can absorb oxygen upon heating even at low temperature below 600 °C while it is saturated with oxygen under subsequent cooling after exposure to argon with low oxygen content. The uptake of oxygen by Ti_3AlC_2 below 600 °C resulted in a greater weight gain (1.86%) upon heating than that (1.57%) under cooling.

Figure 3a shows the secondary electron image of the white cotton-like matter separated from the Ti_3AlC_2 specimen heated to 1460 °C in Ar. It can be seen that the white cotton-like matter consists of a number of balls around which nanoscale needles are distributed uniformly. By using EDS equipped in the field emission scanning electron microscope, the matter was proved to be Al_2O_3 as indicated by the EDS spectrum shown in Figure 3b.

As described above, beneath the white cotton-like matter, the color of the powders changed to black. The black powders were examined by SEM/EDS. Figure 4a and b show the secondary electron images of the black powders. It can be seen that aligned submicropores are distributed on the particulates. Those aligned pores are regarded as the result of selective oxidation of Al in Ti_3AlC_2, which yields the transformation of Ti_3AlC_2 into TiC_x and Al_2O_3. Because the density of TiC_x is larger than that of Ti_3AlC_2, so the transformation process from

(23) Rao, Y. K. *Stoichoimetry and Thermodynamics of Metallurgical Processes*; Cambridge University Press: Cambridge, U.K., 1985.
(24) Turkdogan, E. T. *Physical Chemistry of High-Temperature Technology*; Academic Press: New York, 1980.
(25) Barin, I.; Knacke, O. *Thermochemical Properties of Inorganic Substances*; Springer-Verlag: Berlin, 1973.
(26) Wang, X. H.; Zhou, Y. C. *J. Mater. Chem.* **2002**, *12*, 2781.
(27) Bellucci, A.; Gozzi, D.; Nardone, M.; Sodo, A. *Chem. Mater.* **2003**, *15*, 1217.

Ti_3AlC_2 into TiC_x would cause shrinkage in volume and pores emerged on the oxidized particles. Considering aluminum atoms in nano-laminate Ti_3AlC_2 exist in a planar manner, there is little doubt that the pores distributed on the oxidized particles are aligned. Similar aligned submicropores were also observed by Barsoum and co-workers in the topotactic transformation of Ti_3SiC_2 into a partially and cubic $Ti(C_{0.67}Si_{0.06})$ by the diffusion of Si into molten cryolite.[22] By using EDS, it is demonstrated that oxygen was detected in the regions where aligned submicropores exist in the oxidized particles. In addition to oxygen, the other elements Ti, C, and minor Al were also detected as shown in Figure 5, which suggests that uptake of oxygen by substoichiometric TiC_x took place and consequently titanium oxycarbide formed. It is reported in the literature[28] that the substitution of C with O in TiC does not change its rock salt structure, and the difference in cell parameters between TiC (TiC, $a = 0.43274$ nm)[29] and titanium oxycarbide ($TiC_{0.73}O_{0.27}$, $a = 0.4312$ nm)[27] is quite small. As a result, they show very similar XRD patterns.

At this stage, as selective oxidation of aluminum occurred, the idealized transformation of Ti_3AlC_2 can be written as follows:

$$4Ti_3AlC_2 + (3 + 6y)O_2 = 12TiC_{0.67}O_y + 2Al_2O_3,\ y < 0.33 \quad (1)$$

Just owing to that the aligned pores acted as rapid channels for Al to migrate outward and the migration is a synergic and whole behavior, there was no Al-depletion layer beneath the protective scales for the bulk Ti_3AlC_2 and Ti_2AlC ceramics.[6,7] The advantage in understanding the absence of Al-depletion layer for the bulk Ti_3AlC_2 and Ti_2AlC ceramics is obvious, because Ti_3AlC_2 powders are isolated without continuous providing of Al from substrate, aligned micropores can be observed.

The transformation process from Ti_3AlC_2 into titanium oxycarbide ($TiC_{0.67}O_y$) owing to the selective oxidation of Al into Al_2O_3 is schematically illustrated in Figure 6. For the reason that this transformation process was initiated from the surface, so the reaction rate for Ti_3AlC_2 powders is relatively rapid owing to the high specific surface area, whereas in the case of bulk Ti_3AlC_2 the transformation rate is very slow.

4. Conclusions

Nano-laminate Ti_3AlC_2 was stable up to at least 1460 °C. In addition, transformation of Ti_3AlC_2 into titanium oxycarbide ($TiC_{0.67}O_y$) and Al_2O_3 only took place at the top of the specimen, suggesting that the transformation was induced by the selective oxidation of Al into thermodynamically stable Al_2O_3. Aligned submicropores were observed on the oxidized particles. Those aligned pores acted as the rapid channels through which aluminum atoms could easily migrate outward from the substrate, and consequently, protective scales formed on bulk Ti_3AlC_2 and Ti_2AlC ceramics at high temperatures. Because the migration is a synergic and whole behavior, there is no Al-depletion area beneath the protective scales. Meanwhile, it also provides an alternative route to synthesize nanoscale α-Al_2O_3.

Acknowledgment. This work was financially supported by the National Outstanding Young Scientist Foundation for Y.C.Z. under Grant 59925208, the National Science Foundation of China (NSFC) under Grant 50072034 and 50232040, the '863' program, the IMR Innovative Research Foundation, and Chinese Academy of Sciences.

CM030022V

(28) Ouensanga, A. *J. Less-common Met.* **1979**, *63*, 225.
(29) International Center for Diffraction Data; JCPDS 32-1383.